CNS-resident classical DCs play a critical role in CNS autoimmune disease

David A. Giles,[1,2,3] Patrick C. Duncker,[1,2] Nicole M. Wilkinson,[1] Jesse M. Washnock-Schmid,[1] and Benjamin M. Segal[1,2,4]

[1]Holtom-Garrett Program in Neuroimmunology, Department of Neurology, [2]Graduate Program in Immunology, and [3]Medical Scientist Training Program, University of Michigan, Ann Arbor, Michigan, USA.
[4]Neurology Service, VA Ann Arbor Healthcare System, Ann Arbor, Michigan, USA.

Experimental autoimmune encephalomyelitis (EAE) is an inflammatory demyelinating disease of the central nervous system (CNS), induced by the adoptive transfer of myelin-reactive CD4$^+$ T cells into naive syngeneic mice. It is widely used as a rodent model of multiple sclerosis (MS). The development of EAE lesions is initiated when transferred CD4$^+$ T cells access the CNS and are reactivated by local antigen-presenting cells (APCs) bearing endogenous myelin peptide/MHC class II complexes. The identity of the CNS-resident, lesion-initiating APCs is widely debated. Here we demonstrate that classical dendritic cells (cDCs) normally reside in the meninges, brain, and spinal cord in the steady state. These cells are unique among candidate CNS APCs in their ability to stimulate naive, as well as effector, myelin-specific T cells to proliferate and produce proinflammatory cytokines directly ex vivo. cDCs expanded in the meninges and CNS parenchyma in association with disease progression. Selective depletion of cDCs led to a decrease in the number of myelin-primed donor T cells in the CNS and reduced the incidence of clinical EAE by half. Based on our findings, we propose that cDCs, and the factors that regulate them, be further investigated as potential therapeutic targets in MS.

Introduction

Experimental autoimmune encephalomyelitis (EAE), an autoimmune demyelinating disease of the central nervous system (CNS), is widely used as an animal model of multiple sclerosis (MS). EAE can be induced by the adoptive transfer of highly purified, myelin-reactive CD4$^+$ Th1 or Th17 effector cells into otherwise unmanipulated, syngeneic hosts. Lesion formation in adoptively transferred EAE is triggered when myelin-specific CD4$^+$ T cells access the naive CNS and are reactivated by local antigen-presenting cells (APCs) bearing endogenous myelin peptide/MHC class II (MHCII) complexes (1). The identity of the CNS-resident, lesion-initiating APCs is widely debated. By definition, the cell type in question must express MHCII and costimulatory molecules and possess the machinery necessary to process immunogenic peptides from larger myelin proteins. In order to mediate epitope spreading during clinical relapse and/or progression, a candidate APC would also have to be capable of activating naive CD4$^+$ T cells specific for secondary myelin epitopes and of polarizing them toward encephalitogenic Th1 or Th17 lineages (2).

Microglia have been posited as the critical resident APCs of the CNS (3). It has become increasingly recognized that microglia are heterogeneous, and that distinct subsets may play different roles during the evolution of disease (4). However, the ability of microglia, particularly when in a resting state, to efficiently activate T cells has been questioned by several laboratories (5, 6). Although astrocytes and cerebrovascular endothelium were reported to express MHCII in response to inflammatory stimuli (7, 8), they do not do so during homeostasis, nor do they express molecules necessary for antigenic processing and loading. Furthermore, experiments with reciprocal WT/MHCII$^{-/-}$ bone marrow chimeric mice indicate that induction of EAE by adoptive transfer requires MHCII expression on radiosensitive hematopoietic host cells, while expression on radioresistant nonhematopoietic host cells is dispensable (9).

Several subsets of bone marrow–derived MHCII$^+$ cells normally populate the CNS, including perivascular, meningeal, and choroid plexus macrophages (10). In addition, MHCII$^+$ cells with characteristics of dendritic cells (DCs), based on cell surface marker expression, morphology, and/or ultrastructural characteristics, are normal constituents of the choroid plexus, meninges, and perivascular spaces in the uninjured CNS of both humans and rodents (9, 11–17). These CNS-resident DCs are optimally positioned to interact with infiltrating T cells since the choroid plexus and meninges, as well as CNS parenchymal blood vessels, are important portals of leukocyte entry during EAE and MS (18–21). The lineage(s) and biological properties of putative CNS DCs have yet to be delineated. Genetically engineered mice in which MHCII expression is restricted to CD11c$^+$ cells are susceptible to EAE, suggesting that DCs alone are sufficient to present antigen to encephalitogenic T cells in vivo and, thereby, promote their local expansion and effector functions (9). DCs are generally considered potent APCs, owing to their ability to activate and polarize naive T cells, which have an elevated threshold for T cell receptor (TCR) signaling compared with effector and/or memory T cells. However, the potential role of DCs in EAE pathogenesis is complicated by the fact that DCs are heterogeneous with a range of functional phenotypes, and can even be tolerogenic under certain circumstances (22). It is also unclear whether CNS-resident CD11c$^-$MHCII$^+$ cells can inde-

Authorship note: DAG and PCD are co–first authors.
Conflict of interest: The authors have declared that no conflict of interest exists.

Submitted: July 20, 2018; **Accepted:** September 11, 2018.
Reference information: *J Clin Invest*. 2018;128(12):5322–5334.
https://doi.org/10.1172/JCI123708.

pendently activate encephalitogenic T cells in situ. Indeed, depletion of CD11c$^+$ cells in transgenic mice that express diphtheria toxin receptor (DTR) under control of the CD11c promoter has been variably reported to ameliorate or exacerbate the clinical course of EAE, or to have no impact whatsoever (23, 24).

CD11c$^+$MHCII$^+$ DCs include monocyte-derived DC (moDC) and classical DC (cDC) subsets. A third DC subset, plasmacytoid DCs (pDCs), express low levels of CD11c and MHCII, limiting their ability to present antigen to CD4$^+$ T cells. moDCs are not normally present in healthy parenchymal tissues but differentiate from infiltrating Ly6C^{hi} monocytes in the setting of inflammation. We and others have previously shown that moDCs accumulate in the CNS during EAE and that their depletion or inactivation ameliorates clinical disability (25–28). However, the fact that moDCs primarily emerge in the setting of active inflammation precludes their role in lesion initiation. Unlike moDCs, cDCs populate lymphoid, as well as some nonlymphoid, tissues in the steady state. They are derived from a common DC precursor, called the pre-DC, in the bone marrow and expand in response to the hematopoietin FMS-like receptor tyrosine kinase 3 (FLT3) ligand. DCs that have been detected in the murine CNS under physiological conditions are FLT3 dependent, differentiate from transferred pre-DCs, and express a transcriptome consistent with cDCs (29). FLT3 ligand antagonists suppress, while FLT3 ligand agonists exacerbate, clinical EAE, suggesting that cDCs can modulate disease severity (9, 30). However, the ability of CNS-resident cDCs to directly stimulate and polarize myelin-reactive T cells in vivo, and their relative importance in EAE pathogenesis by comparison with infiltrating moDCs or other APC subsets, have yet to be elucidated.

Detailed in vivo studies of moDCs and cDCs have been undermined by a dearth of distinguishing cell surface markers. It was recently reported that CD88 (complement 5a receptor 1 [C5ar1]) and CD26 (dipeptidyl peptidase 4 [DPP4]), an enzyme involved in peptide hydrolysis, are reciprocally expressed by moDCs and cDCs (31). The transcription factor ZBTB46 has also been identified as a singular marker of cDCs in mice and humans (32, 33). These molecules are not exclusive to DCs but are useful in delineating CD11c$^+$ DC lineages. In the present study, we use the above markers to investigate the heterogeneity of DCs during EAE. We detect both moDCs and cDCs in the inflamed target organ but demonstrate that CNS cDCs are uniquely capable of processing immunogenic peptides from larger myelin fragments and activating myelin-specific naive, as well as effector, CD4$^+$ T cells. We found that cDCs are present in the naive CNS and that selective depletion of that subset reduces the incidence of EAE. Hence, cDCs play an important role in disease initiation. Collectively, our data suggest that cDCs, and the factors that regulate them, be investigated as potential therapeutic targets in patients with MS, particularly in those individuals who are not responsive to currently available disease-modifying therapies.

Results

cDCs, as well as moDCs, are present in EAE infiltrates. In order to characterize APC subsets that accumulate in the CNS during EAE, we performed flow cytometric analysis on brain and spinal cord mononuclear cells isolated at the time of peak clinical severity. MHCII$^+$ cells in the brain included CD45^{int}CD11b^{int} microglia, CD45^{hi}CD11b$^+$CD11c$^-$ monocytes/macrophages, CD19$^+$ B cells, and CD45^{hi}CD11c$^+$ DCs (Figure 1A and data not shown). Spinal cord infiltrates had a similar cellular composition (data not shown). The CNS DC population was composed of both CD88$^-$CD26$^+$ cells, consistent with cDCs, and CD88$^+$CD26$^-$ cells, consistent with moDCs (Figure 1A, top right panel). Microglia and macrophages/monocytes expressed CD88 but not CD26 (Figure 1A, bottom panels). We also detected CD26$^+$ pDCs; however, the majority of pDCs were MHCII$^-$, and pDCs constituted less than 5% of the MHCII$^+$CD26$^+$ population in the inflamed CNS (Supplemental Figure 1; supplemental material available online with this article; https://doi.org/10.1172/JCI123708DS1). In order to confirm the lineages of the CD26$^+$ versus CD88$^+$ CNS DC subsets, we performed transcriptional profiling. The CD26$^+$ DC cohort expressed high levels of genes identified by the Immunological Genome Project (ImmGen) (34) as core cDC transcripts, including *Amica1*, *Ccr7*, and *Kit*, while the CD88$^+$ DC cohort expressed markers associated with monocyte-derived cells, including *Slc11a1* (35), *CD84* (36), and *Bst1* (37) (Figure 1B). CNS CD26$^+$ DCs expressed elevated levels of *Flt3* and *Tlr3*, while CD88$^+$ DCs expressed high levels of *Tlr4*, which mirrors the expression of those stimulatory molecules by peripheral cDCs and moDCs, respectively (Figure 1B, right panel) (38). The designation of CNS CD11c$^+$CD26$^+$ cells as cDCs was corroborated by their selective expression of the transcription factor ZBTB46, as demonstrated via intracellular staining and flow cytometry (Figure 1C). Similarly, CD11c$^+$CD26$^+$, but not CD11c$^+$CD88$^+$, cells isolated from *Zbtb46-gfp* reporter mice at peak EAE were GFP$^+$ (Figure 1D).

CNS cDCs are highly efficient APCs. We next compared the ability of CNS cDCs and moDCs to present antigen to myelin-specific CD4$^+$ T cells ex vivo. MHCII$^+$CD11c$^+$ CD88$^+$ moDCs and CD26$^+$ cDCs were FACS-sorted from the CNS at peak EAE and cocultured with naive CD4$^+$ T cells that express a transgenic T cell receptor specific for the myelin oligodendrocyte glycoprotein $(MOG)_{35–55}$ peptide (2D2 cells) (39). 2D2 cells underwent multiple rounds of proliferation, upregulated the activation marker CD44, and expressed intracellular IFN-γ and/or granulocyte-macrophage CSF (GM-CSF) upon coculture with $MOG_{35–55}$ peptide and CNS cDCs (Figure 2, A and B). In contrast, 2D2 cells neither proliferated, upregulated CD44, nor expressed effector cytokines when cocultured with $MOG_{35–55}$ and CNS moDCs. Similar results were obtained with cDCs and moDCs sorted from the spleens of the same mice (data not shown). 2D2 cells did not express FoxP3 under any of the culture conditions. In order to determine whether CNS cDCs could process immunogenic epitopes from larger myelin proteins, we repeated the APC assays using a longer fragment of MOG ($MOG_{1–125}$) as antigen. CNS cDCs were able to process MOG protein and activate 2D2 cells, whereas their moDC counterparts were incompetent (Figure 2, A and B). The superior APC properties of CNS cDCs over moDCs are not antigen specific, since only the former were able to activate OVA-specific TCR-transgenic OT-II cells upon coculture in the presence of either OVA peptide or whole ovalbumin protein (ref. 40 and data not shown).

The majority of CD4$^+$ T cells that infiltrate the CNS during EAE or MS are CD44^{hi} effector cells. As a transgenic T cell line, 2D2 cells do not reflect the heterogeneity of encephalitogenic T cells that infiltrate the CNS during EAE, in terms of both TCR affinity

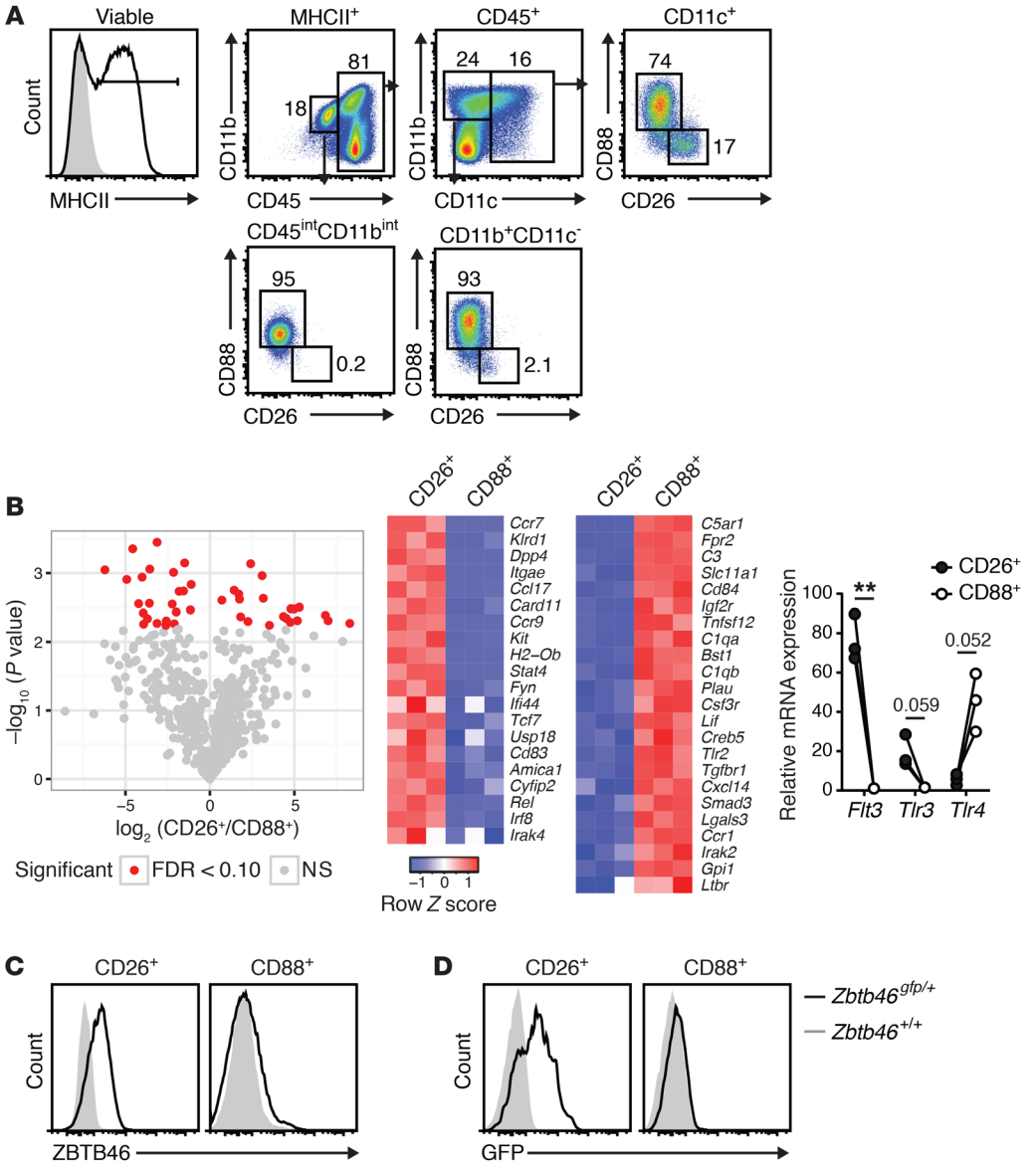

Figure 1. CD26⁺ZBTB46⁺ cDCs accumulate in the CNS during adoptively transferred EAE. EAE was induced by adoptive transfer of WT myelin-primed CD4⁺ Th17 cells into naive syngeneic hosts. (**A**) Brain mononuclear cells were harvested at peak EAE and analyzed by flow cytometry. Dot plots are gated on the population indicated directly above each plot. The numbers indicate percentage of the gated population. The data are representative of 3 experiments. (**B**) MHCII⁺CD11c⁺ CD88⁺ or CD26⁺ cells were purified from the CNS (n = 3 per group) by flow sorting, and gene expression was measured by Nanostring nCounter analysis. Genes with a false discovery rate (FDR) less than 0.10 are identified in the heatmaps. The right panel shows *Flt3*, *Tlr3*, and *Tlr4* mRNA levels in paired DC subsets from individual mice. P values were determined by paired, 2-tailed Student's t test. $^{**}P < 0.01$. (**C** and **D**) Expression of ZBTB46 was measured in MHCII⁺CD11c⁺ CD26⁺ or CD88⁺ brain mononuclear cells, harvested at peak EAE, by flow cytometry. The open histograms reflect intracellular staining with anti-ZBTB46 antibodies (**C**) or GFP expression in cells from *Zbtb46*$^{gfp/+}$ reporter mice (**D**). The shaded gray histograms reflect the isotype (**C**) or nonreporter control (**D**).

and biological properties. To more accurately simulate the local T cell–APC interactions that occur during autoimmune demyelinating disease, we isolated CD4⁺ T cells from the CNS of mice at peak EAE and reconstituted them with purified DC subsets obtained from the same tissues. Notably, CNS cDCs spontaneously induced the proliferation of the CNS-infiltrating effector CD4⁺ T cells in the absence of exogenous antigen, ostensibly because of the presence of endogenous myelin peptide/MHCII complexes on their cell surface (Figure 2C). Proliferation of the effector T cells was enhanced by pulsing of the CNS cDCs with $MOG_{35–55}$. moDCs failed to induce a significant effector T cell response, even when the cocultures were supplemented with $MOG_{35–55}$ (Figure 2C). Taken together, these data demonstrate that cDCs, but not moDCs, are proficient at activating both naive and antigen-experienced myelin-specific T cells.

We next measured a panel of selected cytokines in supernatants from the APC assays. Coculturing 2D2 cells with CNS cDCs, in the presence of either $MOG_{35–55}$ or $MOG_{1–125}$, resulted in the production of IL-2, IL-17A, IFN-γ, and GM-CSF (Figure 2D). Similar results were obtained when CD4⁺ effector T cells, isolated from the inflamed CNS, were cocultured with $MOG_{35–55}$ and CNS cDCs (Figure 2E). In contrast, we did not detect any cytokines in supernatants from cocultures of 2D2 cells and moDCs with MOG peptides (Figure 2D).

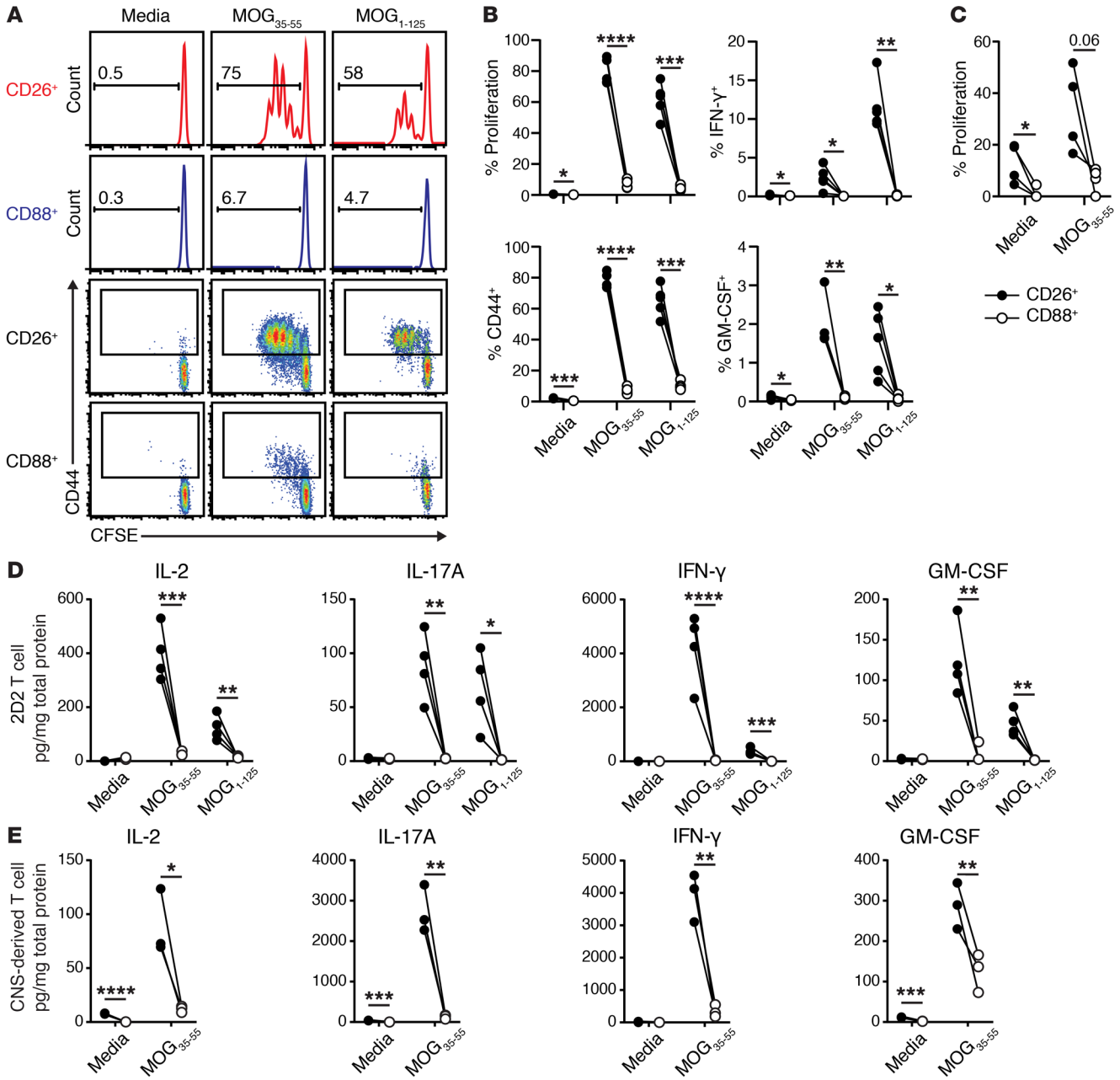

Figure 2. CNS cDCs stimulate naive and effector myelin-specific T cells to proliferate and produce proinflammatory cytokines, while CNS moDCs are incompetent APCs. EAE was induced by active immunization with MOG_{35-55} peptide in CFA. CNS mononuclear cells were harvested at peak disease. $CD26^+$ or $CD88^+$ DC subsets ($CD45^+MHCII^+CD11c^+$) were purified by FACS and cocultured with MOG-reactive T cells in the presence or absence of myelin peptide (MOG_{35-55}) or myelin protein (MOG_{1-125}). (**A**, **B**, and **D**) The CNS DC subsets were cocultured with $CD44^-CD62L^+$ $CD4^+$ T cells that had been isolated from the spleens and lymph nodes of naive 2D2 TCR-transgenic mice. (**A** and **B**) T cell proliferation was measured by CFSE dilution. The percentage of $CD4^+$ T cells that underwent 1 or more division, or that expressed the activation marker CD44, is shown for each group. (**B**) Cytokine production was measured by intracellular flow cytometry. The percentage of cytokine producers among total $CD4^+$ T cells is shown. (**D**) Cytokine levels were measured in culture supernatants via a multiplex Luminex bead-based assay. (**C** and **E**) CNS DC subsets were cocultured with $CD4^+$ T cells isolated from the CNS at the peak of EAE. (**C**) T cell proliferation was measured as in **A**. (**E**) Cytokine levels were measured in culture supernatants via Luminex. (**B**–**E**) Each circle represents a data point generated with CNS DC subsets isolated from a single mouse. Connected circles indicate paired samples from the same mouse. $^*P < 0.05$, $^{**}P < 0.01$, $^{***}P < 0.001$, $^{****}P < 0.0001$ by paired, 2-tailed Student's *t* test. Data in **A**, **B**, and **D**, and in **C** and **E**, are from individual experiments that are representative of 2–4 independent experiments with similar results. $n = 3$–5 mice per group per experiment.

moDCs did elicit production of GM-CSF (but none of the other cytokines in the panel), when cocultured with CNS-infiltrating effector T cells and MOG_{35-55} (Figure 2E). The amount of GM-CSF produced was significantly lower than the amount elicited by CNS cDCs.

We performed APC assays with resident microglia, and splenic and CNS-infiltrating B cells, as a foil to the CNS DC subsets. B cells, isolated from either the CNS or spleen at peak EAE, induced 2D2 cell proliferation in response to exogenous MOG_{35-55} pep-

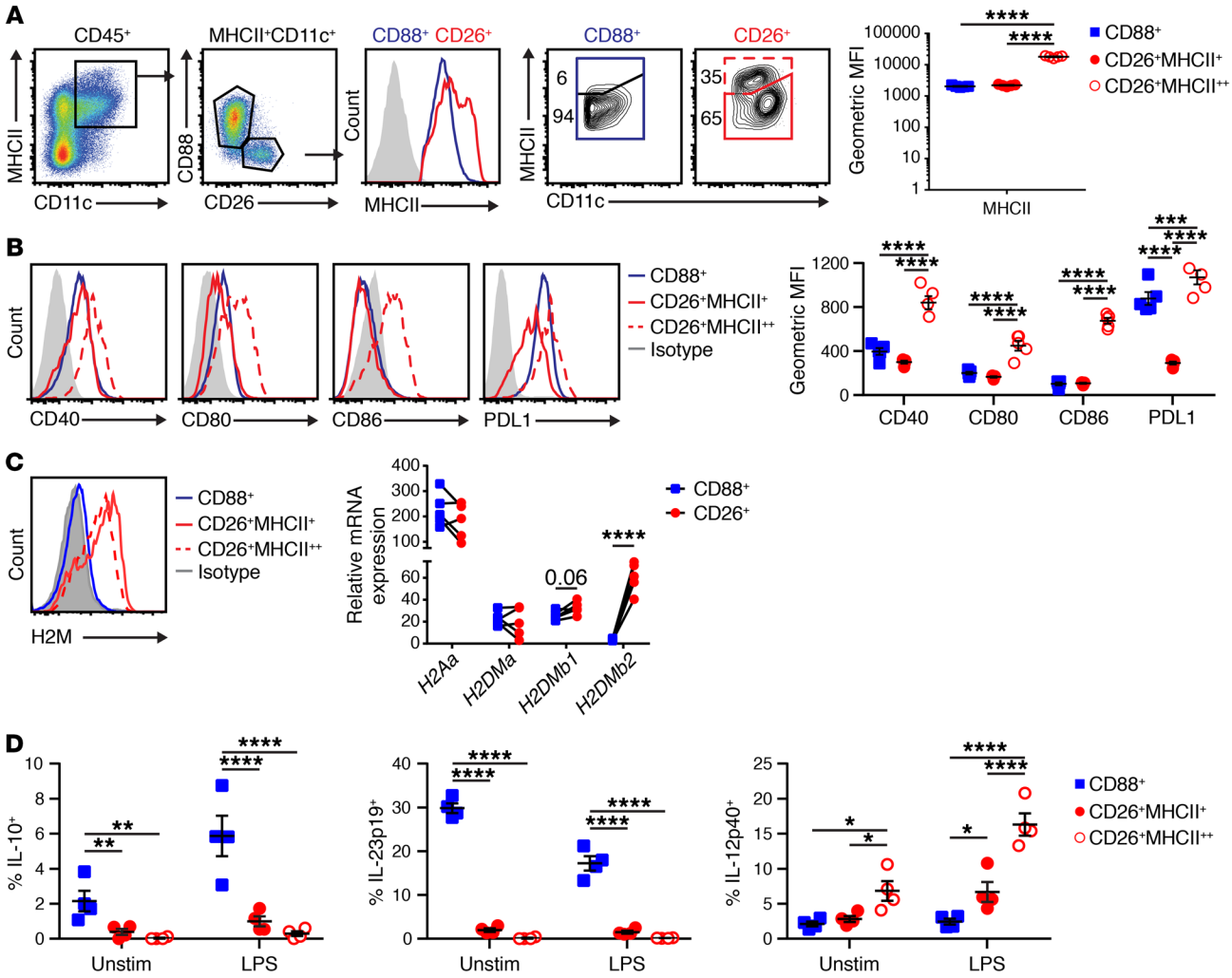

Figure 3. CNS moDCs are deficient in expression of H2M and have a distinct cytokine profile in comparison with CNS cDCs. EAE was induced by adoptive transfer of WT myelin-primed Th17 cells into naive syngeneic hosts. (**A** and **B**) CNS mononuclear cells were isolated at peak clinical severity and subjected to flow cytometric analysis. The geometric mean fluorescence intensity (MFI) of MHCII (**A**) and costimulatory molecules (**B**) was measured on gated DC subsets. (**C**) H2M expression was assessed in CNS DC subsets by flow cytometry (left). The levels of transcripts encoding MHCII and H2M subunits were quantified in FACS-sorted CD88$^+$ and CD26$^+$ CNS DCs via quantitative PCR (right). (**D**) CNS mononuclear cells, isolated from individual mice with EAE, were cultured for 4 hours with brefeldin A, with or without LPS. Cytokine production was assessed by intracellular staining and flow cytometry. The data are shown as the percentage of cytokine-positive cells within the indicated DC population. Each symbol represents a data point generated from a single mouse. Connected symbols indicate paired samples from the same mouse. *$P < 0.05$, **$P < 0.01$, ***$P < 0.001$, ****$P < 0.0001$. Statistical significance was determined using 1-way (**A**) or 2-way (**B** and **D**) ANOVA with Tukey's post hoc test or (**C**) paired 2-tailed Student's t test. n = 3–5 mice per group or condition. All data are representative of at least 2 experiments. All error bars indicate mean ± SEM.

tide (Supplemental Figure 2A). Conversely, they were inefficient at processing and presenting the larger MOG_{1-125} protein to the naive myelin-reactive T cells. CNS-infiltrating B cells induced the spontaneous proliferation of myelin-primed effector T cells, but this was not enhanced by the addition of exogenous antigen (Supplemental Figure 2B). MHCII$^+$CD45^{int}CD11b^{int} microglia did not stimulate the proliferation of either naive or effector T cells, even when cultured with MOG_{35-55} (Supplemental Figure 2, C and D).

cDCs express high levels of H2M molecules. We next investigated the mechanism underlying the disparate APC capacities of CNS cDCs versus moDCs. First, we measured the cell surface density of MHCII molecules on each subset via mean fluorescence intensity (MFI). This analysis revealed the presence of 2 populations within the CNS CD26$^+$ cDC subset that were distinguished by expression of either high (CD11c^{int}MHCII^{++}) or comparable (CD11^{hi}MHCII$^+$) levels of MHCII in comparison with their CD88$^+$ counterparts (Figure 3A). The CD26$^+$MHCII^{++} subpopulation also expressed elevated levels of the costimulatory markers CD40, CD80, and CD86 (Figure 3B). In order to determine whether these disparities in MHCII and costimulatory molecule expression translated into functional differences, we performed APC assays with the CNS DC subsets side by side. There was no significant difference in the proliferation of 2D2 cells cocultured with the CD26$^+$ MHCII$^+$ versus CD26$^+$MHCII^{++} cDC subpopulations. Both of the CD26$^+$ cDC subpopulations promoted more 2D2 cell activation than CD88$^+$ moDCs sorted from the same CNS mononuclear suspension (Supplemental Figure 3). We also measured expression of the inhibitory ligand PDL1, and found that it was expressed on

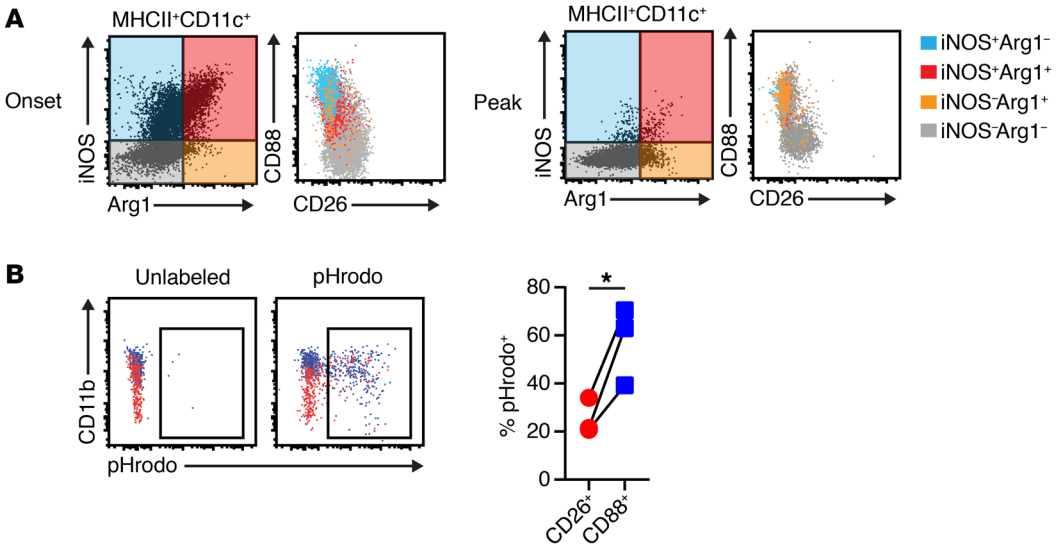

Figure 4. CNS moDCs express iNOS and Arg1 and efficiently phagocytose myelin. (**A**) EAE was induced by active immunization with myelin peptide, and CNS mononuclear cells were isolated at clinical onset (left panels) or peak disease (right panels). Expression of inducible nitric oxide synthase (iNOS) and arginase-1 (Arg1) in CD88$^+$ or CD26$^+$ CNS DCs was assessed by intracellular flow cytometry. All of the dot plots are gated on MHCII$^+$CD11c$^+$ cells. Cells in the CD88 versus CD26 dot plots are color coded based on patterns of iNOS and Arg1 expression. (**B**) EAE was induced by adoptive transfer of WT myelin-primed Th17 cells. Mononuclear cells were isolated from the CNS at the peak of EAE and cultured overnight with unlabeled or pHrodo-labeled purified myelin. Phagocytosis was measured as the percentage of pHrodo$^+$ cells within gated CD26$^+$ or CD88$^+$ DC populations. Each symbol represents a data point generated from a single mouse. Connected symbols indicate paired samples from the same mouse. Data are representative of 2 experiments. *$P < 0.05$ by paired, 2-tailed Student's *t* test. *n* = 3–5 mice per group or condition.

all 3 subsets. Blockade of PDL1 did not rescue myelin-specific T cell activation by CNS moDCs (data not shown). Based on these results, we concluded that heightened MHCII and/or costimulatory molecule expression was not responsible for the superior antigen-presenting capacity of CNS cDCs.

H2M (HLA-DM in humans) is a nonclassical MHC molecule that facilitates antigen loading into the binding groove of MHCII. It functions by catalyzing the exchange of class II–associated invariant chain peptide (CLIP; a space-holding peptide that is inserted into the binding groove during the assembly of MHCII to stabilize its structure) and endosomal peptides (41). H2M-deficient mice are defective in the processing of native MOG for presentation to encephalitogenic T cells and are resistant to EAE, induced by either active immunization or adoptive transfer (42). Therefore, we questioned whether CNS moDCs are incompetent APCs because of reduced expression of H2M. We found that CNS cDCs expressed high levels of H2M protein (Figure 3C, left). Conversely, we did not detect H2M protein in CNS moDCs. In addition, CNS cDCs expressed much higher levels of the transcripts encoding H2M subunits than CNS moDCs (Figure 3C, right). Hence, insufficient processing and binding of immunogenic myelin peptides to MHCII may underlie the relative inability of CNS moDCs to activate encephalitogenic T cells.

cDCs and moDCs have distinct cytokine profiles. In order to further characterize the immunological properties of the CNS DC subsets, we measured intracellular expression of candidate polarizing factors. We observed distinctive cytokine profiles among the DC subsets, in that CD26$^+$ cDCs expressed IL-12p40 following short-term incubation with brefeldin A, while CD88$^+$ moDCs expressed IL-23p19 and IL-10 (Figure 3D). IL-12p40 is a subunit of both IL-12 and IL-23. Production of IL-12p40 by CNS CD26$^+$ cDCs is consistent with their induction of IFN-γ in myelin-reactive T cells (Figure 2, B, D, and E). Measurement of IL-12p35, the second subunit of bioactive IL-12 heterodimer, was limited by available methods. IL-23 is a heterodimer of IL-12p40 and IL-23p19 (43), and polarizes T cells toward IL-17 production and the Th17 phenotype (44). Although CNS CD88$^+$ moDCs express IL-23p19, they would be unable to synthesize bioactive IL-23 in the absence of IL-12p40. This might explain the failure of CNS moDCs to induce IL-17 production upon coculture with myelin-specific T cells (Figure 2, D and E). Instead, CD88$^+$ moDC production of IL-10 may exert a regulatory influence on the inflammatory process. Stimulation of the CNS DC subsets with LPS altered the level, but not the pattern, of cytokine production (Figure 3D).

moDCs efficiently phagocytose myelin. Having established CNS-derived cDCs as superior APCs, we questioned the role of moDCs in neuroinflammatory disease. We recently reported that CD11b$^+$CD11c$^+$ DCs evolve during the course of EAE and shift from a proinflammatory phenotype (denoted by expression of the enzyme inducible nitric oxide synthase [iNOS]) at clinical onset to a noninflammatory or immunosuppressive state (denoted by expression of the alternative enzyme arginase-1 [Arg1]) in anticipation of clinical remission/stabilization (4). During this transition, some of the CNS DCs acquire an iNOS$^+$Arg1$^+$ intermediary phenotype. Our published study did not address the lineage of the CNS DC populations. Upon revisiting this issue, we found that iNOS and/or Arg1 expression is restricted to moDCs throughout the disease course (Figure 4A).

Since the monocyte/macrophage lineage is specialized in phagocytosis, we also compared the capacity of CNS moDCs and cDCs to internalize extracellular myelin. We isolated total CNS

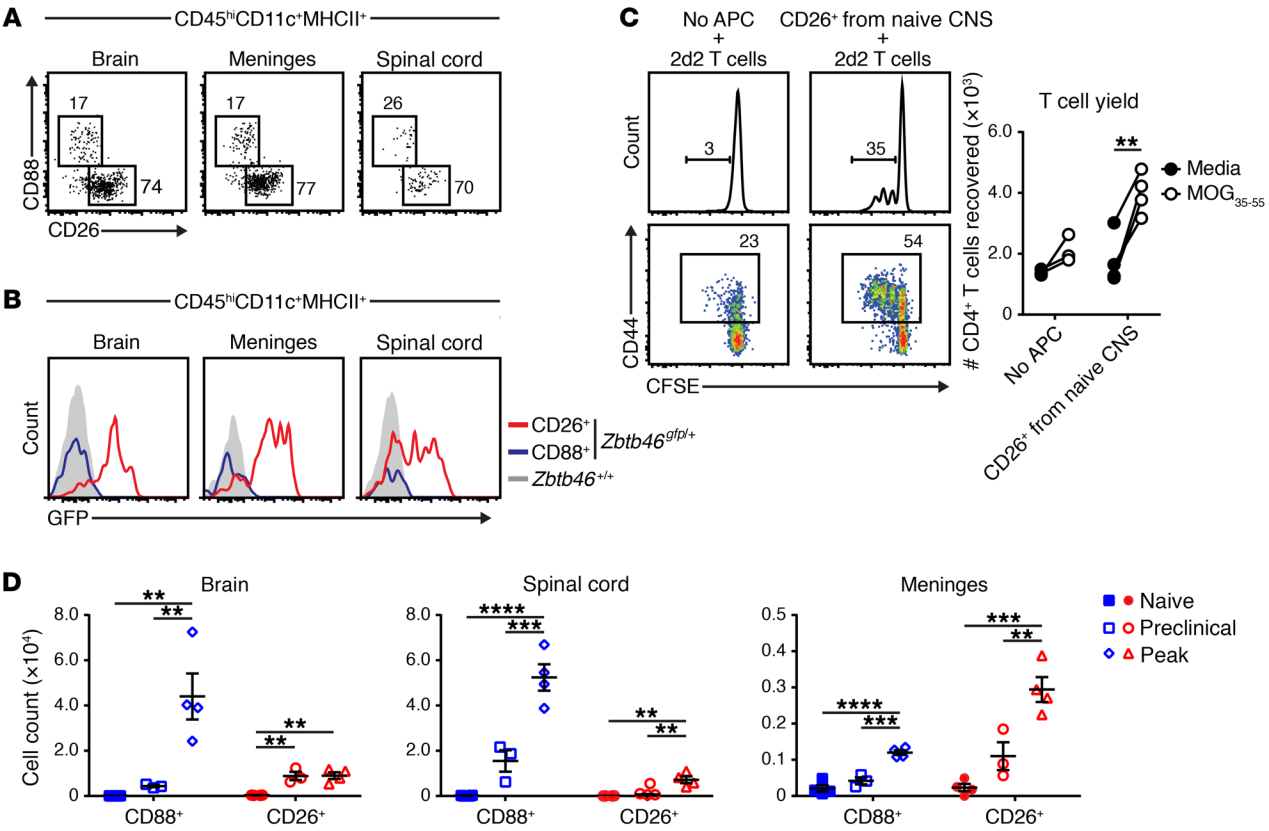

Figure 5. cDCs reside in the naive CNS and expand during EAE. (**A**) Mononuclear cells were isolated from the naive brain, meninges, and spinal cord, and analyzed by flow cytometry. The dot plots are gated on MHCII$^+$CD45^{hi}CD11c$^+$ cells. (**B**) CNS mononuclear cells harvested from naive *Zbtb46*$^{gfp/+}$ reporter mice or *Zbtb46*$^{+/+}$ controls were analyzed for GFP expression, gating on MHCII$^+$CD11c$^+$ DC subsets. (**C**) MHCII$^+$CD11c$^+$CD26$^+$ cDCs were isolated from the naive CNS and cocultured with naive 2D2 transgenic T cells in the presence or absence of MOG peptide. 2D2 cells were also cultured in the absence of APCs as a negative control. 2D2 proliferation was measured by CFSE dilution, and activation by upregulation of CD44 (left). The numbers in the histograms and dot plots represent the percentage of 2D2 T cells that divided or expressed CD44, respectively. Live 2D2 cells were counted at the completion of culture (right). Connected symbols indicate paired samples from the same mouse. (**D**) Cells were isolated from the naive CNS or from the CNS during the preclinical or peak stages of adoptively transferred EAE. CNS DC subsets were quantified by flow cytometry. Each symbol represents a data point generated from a single mouse. $^{**}P < 0.01$, $^{***}P < 0.001$, $^{****}P < 0.0001$. Statistical significance was determined using paired, 2-tailed Student's *t* test (**C**) or 1-way ANOVA with Tukey's post hoc test (**D**). *n* = 3–5 mice per group or condition. All data are representative of at least 2 experiments. Error bars indicate mean ± SEM.

mononuclear cells from mice with EAE and cultured them overnight with purified myelin that had been obtained from a naive mouse and labeled with the pH-sensitive dye pHrodo. In a representative experiment, we detected myelin in the cytoplasm of approximately 55% of CD88$^+$ moDCs compared with approximately 25% of cDCs (Figure 4B). Similar results were obtained when FACS-sorted moDCs and cDCs were cultured independently (data not shown). Myelin phagocytosis by both DC subsets was inhibited by the addition of cytochalasin D, demonstrating dependence on actin polymerization (45) (data not shown). These data indicate that the inability of CNS moDCs to present antigen to myelin-specific T cells is not secondary to a defect in myelin phagocytosis. Moreover, our results suggest potential roles for CD88$^+$ moDCs in modulation of the inflammatory milieu and clearance of myelin debris.

cDCs are present in the naive CNS and expand during autoimmune demyelinating disease. We hypothesized that resident cDCs are the primary APCs encountered by encephalitogenic T cells as they enter the uninflamed CNS, and that cDCs drive T cell activation at the inception of neuroinflammation, and possibly during epitope spreading. In support of this theory, FLT3-dependent, radiosensitive DCs were recently discovered in the meninges under steady-state conditions (16, 29, 46). Similarly, we detected MHCII$^+$CD11c$^+$CD26$^+$ DCs in the naive meninges and brain and, to a lesser extent, in the naive spinal cord by flow cytometric analysis (Figure 5A). The CNS DC population in naive C57BL/6 mice was predominantly CD88$^-$CD26$^+$ (Figure 5A). CD26$^+$, but not CD88$^+$, CD11c$^+$ DCs isolated from the CNS of unmanipulated *Zbtb46-gfp* reporter mice expressed GFP (Figure 5B). MHCII$^+$CD11c$^+$CD26$^+$ cDCs isolated from uninflamed CNS tissues readily activated naive, myelin-specific CD4$^+$ T cells directly ex vivo and enhanced T cell survival during short-term culture (Figure 5C).

Time course studies revealed that cDCs and moDCs progressively expand from baseline through the onset and peak of EAE in every CNS compartment that we examined (Figure 5D). Although cDCs consistently accumulated in the brain and spinal cord in association with increasing neurological disability, their expansion was overshadowed by a dramatic rise in the frequency of moDCs. Consequently, moDCs were the predominant DC subset in the brain and spinal cord by peak disease. In contrast, the frequency of meningeal cDCs exceeded that of moDCs at both the preclini-

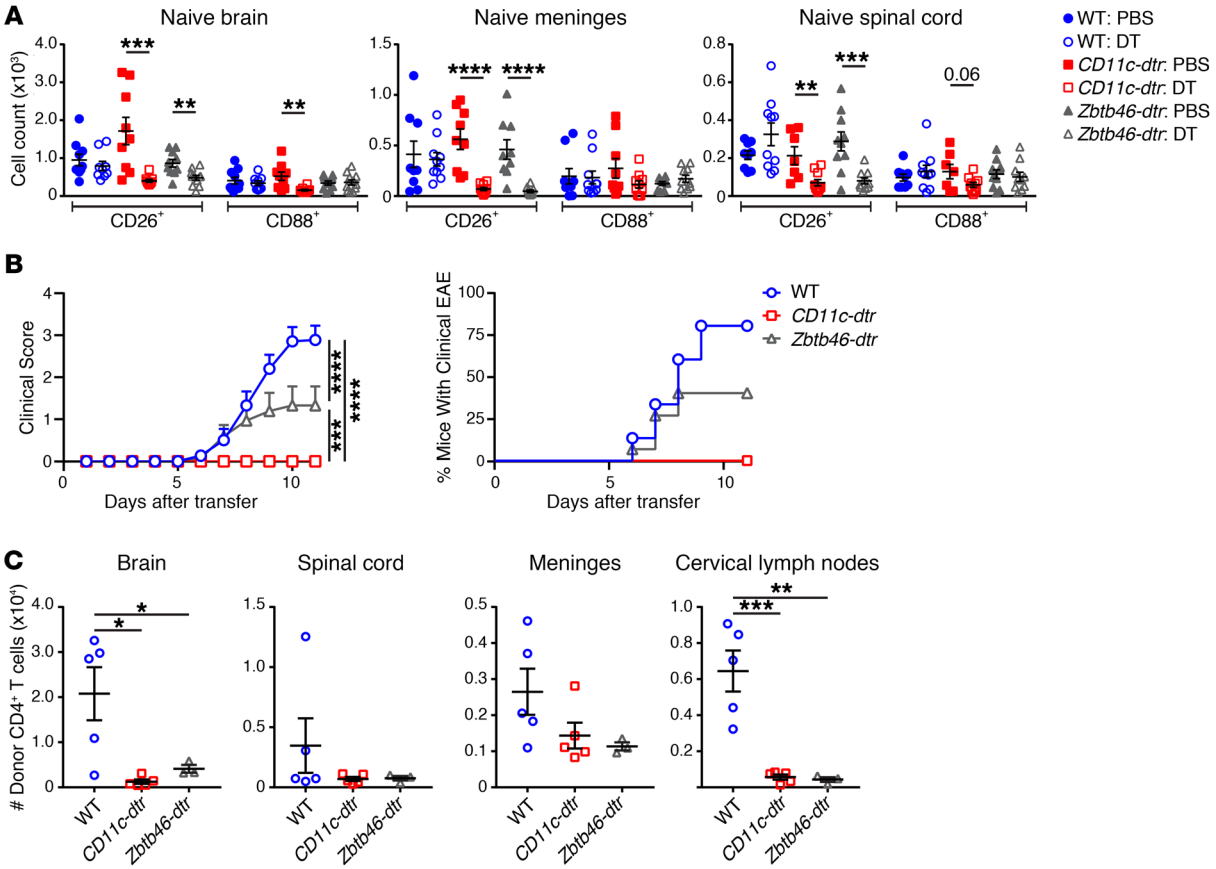

Figure 6. Depletion of cDCs in adoptive transfer recipients results in a decreased number of myelin-primed donor T cells in the CNS and reduces the incidence of clinical EAE. Bone marrow chimeric mice were generated by reconstitution of lethally irradiated CD45.1⁺ hosts with CD45.2⁺ WT, *CD11c-dtr*, or *Zbtb46-dtr* bone marrow cells. (**A**) Naive chimeric mice in each group were treated with DT or PBS for 3 consecutive days. CNS cDC and moDC subsets were quantified by flow cytometric analysis. (**B** and **C**) Chimeric mice were treated with DT as in **A**, and EAE was induced by the adoptive transfer of WT myelin-primed Th17 cells. Daily DT injections were continued throughout the clinical course. (**B**) Mice were monitored on a daily basis and rated for degree of neurological disability by an examiner blinded to the identity of the experimental groups. Clinical scores and incidence are shown for each group. (**C**) Total number of donor (CD45.1⁺) CD4⁺ T cells were enumerated in DT-treated adoptive transfer recipients 1–2 days before expected clinical onset. Each symbol in **A** and **C** represents a data point generated from a single mouse. $^*P < 0.05$, $^{**}P < 0.01$, $^{***}P < 0.001$, $^{****}P < 0.0001$. Statistical significance was determined by unpaired 2-tailed Student's *t* test (**A**), 2-way ANOVA (**B**), or 1-way ANOVA with Tukey's post hoc test (**C**). Data are combined from (**A**) or representative of (**B** and **C**) at least 2 experiments with *n* = 3–15 mice per group or condition. Error bars indicate mean ± SEM.

cal and peak stages of EAE. We and others have found the choroid plexus and meninges to be the initial portal of entry of CNS-infiltrating T cells during EAE (our unpublished observations and refs. 17, 19, 20). Meningeal inflammation is widespread in early as well as progressive stages of MS, and is spatially associated with cortical pathology (14, 47). In a survey of postmortem brain and spinal cord tissues from 11 patients with MS, cells expressing mature DC markers were consistently detected in meningeal infiltrates and were often in close proximity to, or in contact with, proliferating lymphocytes (14). Therefore, the presence of cDCs in the meninges might facilitate the development of nascent demyelinating lesions in the subpial gray matter in addition to the white matter.

cDCs are critical for initiation of EAE. To definitively investigate the role of cDCs in EAE, we used transgenic mice with diphtheria toxin receptor (DTR) expressed under control of the ZBTB46 promoter (*Zbtb46-dtr* mice) (32). ZBTB46 is expressed by endothelial cells as well as DCs (33). Consequently, we generated *Zbtb46-dtr*→WT bone marrow chimeric mice to restrict diphtheria toxin (DT) to the cDC population. In parallel, we generated *CD11c-dtr*→WT bone marrow chimeric mice, which target both cDCs and moDCs (48), as a positive control, and WT→WT bone marrow chimeric mice as a negative control. We optimized the DT dosing strategy to deplete DCs in the CNS before disease induction, and to maintain depletion through the clinical course. Following 3 doses of DT, CD26⁺ cDC counts were reduced by over 50% in the brain, spinal cord, and meninges of both sets of DTR bone marrow chimeras (Figure 6A). As expected, CD88⁺ moDCs were also diminished in the brain and spinal cord of DT-treated *CD11c-dtr*, but not *Zbtb46-dtr*, chimeras.

All of the chimeric mice were treated with 3 daily doses of DT before injection with highly purified myelin-primed Th17 cells. Daily DT injections were continued through the experimental time course. Global depletion of DCs completely prevented clinical EAE in *CD11c-dtr*→WT bone marrow chimeras (Figure 6B). Strikingly, selective depletion of cDCs in *Zbtb46-dtr*→WT chimeras reduced the incidence of clinical EAE by half in comparison with the WT→WT chimeras (40% vs. 80%). Histological findings reflected the clinical scores in that there was no evidence of CNS

parenchymal inflammation or tissue damage in spinal cord sections from *Zbtb46-dtr*→WT mice that remained free of neurological deficits (Supplemental Figure 4). In fact, we did not detect any MHCII$^+$ APCs in those sections. The susceptibility of some of the DT-treated *Zbtb46-dtr*→WT mice to EAE may reflect incomplete cDC depletion, as a small number of CD11c$^+$CD26$^+$ cells persisted in the CNS of DT-treated mice (Figure 6A). DT treatment resulted in decreased numbers of donor CD4$^+$ T cells in the brain, spinal cord, meninges, and CNS-draining cervical lymph nodes of *Zbtb46-dtr*→WT, as well as *CD11c-dtr*→WT, adoptive transfer recipients (Figure 6C). Collectively, our data indicate that cDCs promote the accumulation/expansion of myelin-reactive T cells in the CNS during the effector stage of EAE, thereby increasing susceptibility to clinical disability. The *Zbtb46-dtr*→WT mice that did develop disease had a similar day of onset, maximum score, and degree of weight loss compared with symptomatic WT→WT adoptive transfer recipients (Supplemental Figure 5 and data not shown). This suggests that cDCs play a pivotal role in the inception of the neuroinflammatory response, but that other APC subsets, such as infiltrating B cells, might be able to perpetuate disease activity thereafter.

Discussion

The current study adds to a growing body of literature that challenges the traditional portrayal of the uninjured CNS as an immune-privileged site. Numerous laboratories have documented the presence of a network of MHCII$^+$ innate immune cells, many of which have DC characteristics, in human, as well as rodent, brain and spinal cord under steady-state conditions (11, 15–17). These cells are concentrated in the meninges, choroid plexus, and perivascular space, regions that interface with the periphery, where they are optimally positioned to serve as sentinels and first responders to foreign threats. The possibility that the same leukocytes could be subverted to support autoimmune neuroinflammation is supported by the fact that DCs are enriched in perivascular infiltrates within MS white matter lesions as well as in the meninges overlying cortical lesions (13–15).

Two recent studies suggested that a population of DCs normally present in the healthy mouse meninges and choroid plexus is of the cDC lineage (16, 29). Parabiont experiments indicate that CNS-resident DCs originate from a pre-DC bone marrow precursor and have a half-life of 5 to 7 days (29). However, the role of those cells in autoimmune demyelination was not addressed. The current study corroborates these earlier findings by demonstrating that the dominant DC population in the uninflamed CNS expresses markers and transcripts typical of cDCs (Figures 1 and 5). Our data indicate that CD26$^+$ZBTB46$^+$ DCs are unique among CNS APC subsets in their ability to process immunogenic peptides from larger myelin fragments and activate myelin-specific naive, as well as effector, CD4$^+$ T cells to proliferate and produce proinflammatory cytokines (Figure 2). Most importantly, selective depletion of cDCs led to a reduction in the frequency of transferred myelin-primed CD4$^+$ T cells in the meninges, brain, spinal cord, and cervical lymph nodes, and significantly lowered the incidence of clinical EAE (Figure 6).

DT treatment of *Zbtb46-dtr*→WT adoptive transfer recipients targets cDCs in the periphery as well as in the CNS. However, we believe that cDC depletion in the CNS is most likely responsible for the results shown in Figure 6B. This is supported by prior evidence that MOG-specific donor T cells, analyzed via flow cytometry at serial time points following adoptive transfer, first upregulate activation markers and proliferate within the CNS, as opposed to peripheral lymphoid tissues, 1–2 days before expected clinical onset (our unpublished observations). Our current data demonstrate that cDCs support the expansion/survival of encephalitogenic T cells within the CNS and play an important role in disease initiation (Figure 6, B and C). An analogous role of CNS DCs as APCs in the pathogenesis of human autoimmune demyelinating disease is suggested by the presence of myelin-laden cells expressing mature DC markers in close proximity to, or in contact with, proliferating lymphocytes within active MS lesions, as well as in the overlying meninges (15). The choroid plexus and meninges have been increasingly recognized as portals of entry for the infiltration of encephalitogenic T cells into the CNS (18–21). Furthermore, physical interactions between acutely activated myelin-reactive T cells and perivascular phagocytes have been directly visualized within the meningeal space at EAE onset using 2-photon microscopy (21, 49). We found that cDCs accumulate rapidly in the meninges during EAE (Figure 5D). We are currently investigating whether activated encephalitogenic T cells drive the proliferation and maturation of CNS cDCs, possibly via production of FLT3 ligand and/or GM-CSF (50).

Deficiency in H2M impedes endocytic processing and the loading of MHCII molecules with native peptides (51). Hence, low H2M expression may be, in part, responsible for the inability of $MOG_{1–125}$-pulsed CNS moDCs to activate MOG-reactive T cells (Figure 2). In support of that hypothesis, it was previously shown that APCs isolated from H2M-deficient mice are unable to process whole recombinant MOG protein into immunogenic epitopes (42, 52). We found that $MOG_{35–55}$-pulsed CNS moDCs are also poor APCs. This observation is consistent with published studies that show APCs from H2M-deficient C57BL/6 mice to be impaired in the presentation of short peptides (including $MOG_{35–55}$), as well as whole proteins, to CD4$^+$ T cells (42, 51, 53). The inefficient presentation of exogenous peptides by H2M-deficient APCs may reflect the need for those peptides to displace high-affinity CLIP peptides, which are bound to cell surface MHCII at an elevated density in the absence of H2M (51). H2M-independent pathways undoubtedly also contribute to APC dysfunction of CNS moDCs. Based on the data in Figure 4, moDC production of immunosuppressive cytokines might represent one such pathway.

The success of anti-CD20 B cell–depleting monoclonal antibodies in suppressing MS lesion development and clinical exacerbations underscores the importance of B cells in MS pathogenesis (54). These reagents spare plasma cells, and therapeutic responsiveness does not correlate with a reduction in circulating or cerebrospinal fluid antibody levels, indicating an antibody independent mechanism of action (55). A leading hypothesis is that B cell depletion ameliorates relapsing MS by limiting antigen presentation to encephalitogenic T cells. Meningeal B cell follicles have been discovered adjacent to large subcortical lesions in some patients with secondary progressive MS (56). CD3$^+$ T cells are a regular component of the meningeal follicles, raising the possibility that B cells also serve as APCs in that context (57). Our data are consistent with a potential role of B cells as APCs in EAE. B cells isolated from the CNS during EAE were able to present exog-

enous $MOG_{35–55}$ peptide to autoreactive T cells and stimulate their proliferation ex vivo (Supplemental Figure 2). However, in contrast to CNS cDCs, they were inefficient at processing larger MOG proteins for presentation of immunogenic epitopes. This may be explained by the different pathways used by B cells to acquire peptide versus protein antigen. Protein antigen uptake by B cells is primarily mediated through the B cell receptor (58), such that larger myelin fragments might only be efficiently internalized by myelin-specific B cells. However, the frequency of myelin-specific B cells is highly variable in MS, and appears to be low at early time points in EAE (59). In fact, we found that B cells, isolated from the CNS at EAE onset or peak, failed to phagocytose pHrodo-labeled myelin ex vivo (data not shown). Based on these collective data, we speculate that infiltrating B cells can promulgate neuroinflammation in the setting of established autoimmune demyelinating disease, once myelin peptides are released into the CNS microenvironment via proteolysis. Conversely, the ability of CNS cDCs to process large myelin peptides/proteins for presentation to naive T cells may make them uniquely qualified to serve as APCs when antigen load is low. In support of that theory, encephalitogenic donor T cells are incapable of initiating neuroinflammation in naive adoptive transfer recipients when polyclonal B cells are the sole APCs, unless the precursory frequency of MOG-specific B cells is artificially heightened (60). We have previously shown that CNS-infiltrating myeloid cells, including $CD11c^+$ DCs, shift from a proinflammatory phenotype during early EAE to an alternatively activated phenotype immediately prior to clinical remissions, which correlates with changes in APC function (4). In future studies we plan to investigate how APCs evolve, on the cellular subset as well as the population level, across successive stages of EAE.

Despite the significant advances that have been made in MS therapeutics over the past 15 years, none of the medications approved for the management of MS, including anti-CD20 monoclonal antibodies, are cures, and none are effective in all patients. Up to the present, pharmaceutical development has focused on lymphocytes, and myeloid cells have largely been ignored. We and others have shown that the pathological mechanisms that drive CNS injury in MS are diverse, and that the relative contribution of specific cytokine pathways and immune effector cell subsets can vary from one patient to another (61, 62). Such differences may translate into different patterns of therapeutic responsiveness to individual disease-modifying therapies. For example, B cell–targeting approaches may be particularly effective in MS patients who harbor a high frequency of anti-myelin antibody expressers in their B cell repertoire, which would favor the uptake and presentation of myelin antigens by B cells (63). Conversely, cDC-modulating agents might be effective in individuals who are early in the disease course, when there is a lower lesion burden and less myelin breakdown, thereby limiting the accessibility of immunogenic peptides to B cells and lending a competitive advantage to CNS-resident cDCs as APCs. We would argue that inactivation of cDCs in some individuals with MS might abort the escalation of neuroinflammation and have long-lasting benefits. Furthermore, the discovery of myelin-laden DCs in MS lesions in chronic progressive, as well as recently diagnosed, patients raises the possibility that cDC targeting might be therapeutically beneficial over a broad range of MS clinical subsets and disease stages (15, 47, 56).

Methods

Mice. C57BL/6 and B6.Ly5.1 mice were from Charles River Laboratories. *Zbtb46-gfp*, *Zbtb46-dtr*, *CD11c-dtr*, and 2D2 TCR-transgenic mice were from The Jackson Laboratory. Both male and female mice, age 6–12 weeks, were used in experiments. All mice were bred and maintained under specific pathogen–free conditions at the University of Michigan.

Induction and assessment of EAE. For adoptive transfer, C57BL/6 mice were subcutaneously immunized over the flanks with 100 μg $MOG_{35–55}$ (Bio-Synthesis) in CFA (Difco). At 10–14 days after immunization, the draining lymph nodes (inguinal, brachial, and axillary) were collected and cultured for 96 hours in the presence of 50 μg/ml $MOG_{35–55}$, 8 ng/ml IL-23 (R&D Systems), 10 ng/ml IL-1α (PeproTech), and 10 μg/ml anti–IFN-γ (clone XMG1.2, BioXcell). At the end of culture, $CD4^+$ T cells were purified with CD4 positive selection magnetic beads (Miltenyi), and 3×10^6 to 5×10^6 $CD4^+$ T cells were transferred i.p. into naive recipients. For active EAE, mice were immunized as above and injected with 300 ng of pertussis toxin (List Biological) on days 0 and 2 after immunization. EAE was assessed by a clinical score of disability: 1, limp tail; 2, hind-limb weakness; 3, partial hind-limb paralysis; 4, complete hind-limb paralysis; and 5, moribund state.

Cell isolation. Mice were anesthetized with isoflurane and perfused with PBS. Meninges were isolated by removal of the calvarium, placement of the calvarium in a dish with PBS, and stripping of the meninges from the inner surface. The meninges tissue and loosely adherent cells released in the PBS were collected, pelleted, and incubated in a solution of HBSS with 1 mg/ml collagenase A (Roche) and 1 mg/ml DNase I (Sigma-Aldrich) for 20 minutes at 37°C. The meninges were then passed through a 70-μm mesh filter to remove debris and generate a single-cell suspension. The brain was removed from the skull, and the spinal cord was flushed from the spinal column with PBS. The brain and spinal cord were homogenized with an 18-gauge needle in the collagenase solution and incubated at 37°C for 20 minutes. Mononuclear cells were separated from myelin with a 27% Percoll solution (GE Healthcare). Spleens were isolated and passed through a 70-μm mesh filter to generate a single-cell suspension. Red blood cells from the spleen were lysed by a brief incubation in ACK lysis buffer (Quality Biological) followed by a wash in PBS.

Cytokine production by DC subsets. Mononuclear cells were isolated as above and cultured with brefeldin A (BFA; 10 μg/ml) or BFA plus LPS (1 μg/ml) for 4 hours. At the end of culture, cells were collected and stained for cytokines by intracellular flow cytometry.

Ex vivo cultures. Mononuclear cells were isolated as above, and DC subsets, microglia, and B cells were FACS-sorted from the CNS and spleen according to the indicated surface markers. For purification of naive $CD4^+$ T cells, lymph nodes and spleen were collected from naive 2D2 TCR-transgenic mice. $CD4^+$ T cells were enriched by positive selection with magnetic beads (Miltenyi), and naive T cells were further purified by flow sorting for live $CD4^+CD44^-CD62L^+$ T cells. For purification of effector T cells, mononuclear cells from the CNS were flow-sorted for live $CD45^+CD11b^-CD3^+CD4^+MHCII^-$ T cells. T cells were labeled with CFSE according the manufacturer's instructions (Thermo Fisher Scientific). APCs and T cells were cocultured for 96 hours at a ratio of 1:20 (typically 5,000 myeloid cells with 95,000 T cells) with media, myelin peptide ($MOG_{35–55}$ peptide, Biosynthesis), or myelin protein ($MOG_{1–125}$, Anaspec). At the end of culture, cells were cultured with PMA (50 ng/ml), ionomycin (2 μg/ml), and BFA (10 μg/

ml) for 4 hours to stimulate cytokine production. Cells were collected and stained for activation by surface markers and cytokine production by intracellular staining.

Multiplex cytokine analysis. Cytokine levels were measured by Luminex multiplex bead-based analysis (Millipore) using the Bio-Plex 200 system (BD Biosciences) according to the manufacturer's protocols. Total protein was measured via Bradford assay (Thermo Fisher Scientific) and used to normalize analyte concentrations to total protein.

Phagocytosis. Myelin was purified from the naive mouse brain by ultracentrifugation as previously described (64). Purified myelin was conjugated to the pH-sensitive dye pHrodo Red, succinimidyl ester (Thermo Fisher Scientific), per the manufacturer's protocol. Mononuclear cells were isolated from the CNS at the peak of adoptive EAE and cultured overnight with the unlabeled or pHrodo-labeled myelin (1 μg/200 μl). Cells were collected, washed, and stained for flow cytometry. Phagocytosis was determined by pHrodo Red fluorescence.

Flow cytometry. Cells were labeled with fixable viability dye (eFluor506, eBioscience), blocked with anti-CD16/32 (clone 2.4G2, hybridoma, ATCC), and stained with fluorescent antibodies. For intracellular staining of cytokines and enzymes, cells were fixed with 4% paraformaldehyde, permeabilized with 0.5% saponin, and stained with fluorescent antibodies. For intracellular staining of ZBTB46, cells were fixed and permeabilized with the Transcription Factor Buffer Set (BD Pharmingen). Data were acquired using a FACSCanto II flow cytometer or FACSAria III flow sorter (BD Biosciences) and analyzed with FlowJo software (Tree Star). Cells were sorted with a FACSAria III flow sorter (BD Biosciences).

Antibodies. The following antibodies were obtained from BD Biosciences: αH2M (2E5A), APC-Cy7-(αIFN-γ [XMG1.2], αLy6G [1A8]), biotin-(α-rat IgG1 [RG11/39.4]), FITC-(αCD40 [HM40-3], αCD62L [MEL-14], α-rat IgG1 [RG11/39.4]), and PE-(αCD4 [GK1.5 and RM4-5], αZBTB46 [U4-1374]). The following antibodies were obtained from BioLegend: APC-(αCD26 [H194-112], αCD88 [20/70]), FITC-(αCD26 [H194-112]), biotin-(αCD88 [20/70]), PE-(αCD88 [20/70], αPD-L1 [10F.9G2]), and PE-DAZZLE-(αCD11c [N418]). The following antibodies and reagents were obtained from Thermo Fisher Scientific: APC-(αCD19 [MB19-1], αCD44 [IM7], αIL-23p19 [fc23cpg], streptavidin), APC-Cy7/APC-eF780-(αCD11b [M1/70], αCD45.2 [104], αMHCII [M5/114.15.2]), biotin-(αI-Ab [AF6-120.1]), BV510-(αCD45 [30F11], αCD45.1 [A20]), eF450-(αCD4 [RM4-5]), eF700-(streptavidin), FITC-(αCD45.2 [104], αCD317 [eBio927], αMHCII [M5/114.15.2], streptavidin), PE-(αCD86 [GL1], αIL-10 [JES5-16E3], αGM-CSF [MP1-22E9]), PE-Cy7-(αCD11b [N418], streptavidin), PE-eF610-(αiNOS [CXNFT]), PerCP-Cy5.5-(αCD11c [N418], αIL-12p40 [C17.8], αMHCII [M5/114.15.2]), PerCP-eF710-(αI-Ab [AF6-120.1]), and V506 Fixable Viability Dye. The following antibodies were obtained from R&D Systems: αArg1 (sheep IgG) and FITC-(αArg1 [sheep IgG]). Donkey α-sheep–Alexa Fluor 488 was obtained from Life Technologies.

Nanostring gene expression analysis and quantitative PCR. Sorted cells were resuspended in RLT buffer (QIAGEN), and cell lysates were directly analyzed for expression of 750 immune-related genes with the nCounter PanCancer Immune Panel (Nanostring Technologies). Data were processed using the nSolver Analysis Software by normalization to the geometric mean of positive controls and housekeeping genes. R was used to perform paired Student's *t* tests and calculate Benjamini and Hochberg's false discovery rate, comparing the gene expression of the $CD26^+$ and $CD88^+$ populations. Cells used to confirm the Nanostring results via quantitative PCR were resuspended in RLT buffer before QIAGEN RNeasy RNA purification. Relative mRNA levels were quantified by SYBR Green quantitative PCR performed on an iQ Thermocycler (Bio-Rad).

Bone marrow chimeras. B6.Ly5.1 ($CD45.1^+$) congenic hosts were lethally irradiated with 13 Gy split into 2 doses and reconstituted by tail vein injection of 4×10^6 $CD45.2^+$ bone marrow cells from WT, *CD11c-dtr*, or *Zbtb46-dtr* donors. Mice were allowed to reconstitute for 6 weeks prior to use.

DT ablation. Diphtheria toxin (DT; Sigma-Aldrich) was administered in 2 stages. Three daily doses of 1 μg/20 g mouse (50 μg/kg) in 200 μl of PBS were given i.p. prior to the assessment of DC depletion or to the induction of EAE. Daily doses of 100 ng/20 g mouse (500 ng/kg) in 200 μl of PBS were given i.p. starting on the day of adoptive transfer and continued until the end of the experiment.

Histology. Spinal columns were harvested from mice perfused intracardially with 1× PBS and 4% paraformaldehyde, post-fixed with 4% paraformaldehyde, decalcified with 0.5 M EDTA, cryopreserved with sucrose, and embedded in OCT for cryosectioning. Twelve-micrometer sections were stained with the following primary antibodies: rat anti-$MBP_{82–87}$ (Millipore) and biotinylated rat anti-MHCII (Thermo Fisher Scientific). Avidin/biotin block (Thermo Fisher Scientific) was used to prevent streptavidin binding to endogenous biotin. Normal goat serum (Sigma-Aldrich) was used to block nonspecific binding of secondary goat anti-rat IgG–Alexa Fluor 488 (Thermo Fisher Scientific). Streptavidin-APC (Thermo Fisher Scientific) was used to visualize bound biotinylated anti-MHCII. Confocal images were acquired using an Olympus IX83 with Fluoview 31 software.

Statistics. Statistical analysis was performed in GraphPad Prism (version 7) using paired or unpaired 2-tailed Student's *t* test, or 1-way or 2-way ANOVA with correction for multiple comparisons with Tukey's post hoc test, as indicated in the legends. Disease curves were compared by 2-way ANOVA. Outliers were identified by ROUT analysis and removed when indicated. A P value less than 0.05 (*) was considered significant; $^{**}P < 0.01$, $^{***}P < 0.001$, and $^{****}P < 0.0001$.

Study approval. All animal experiments were performed in accordance with an IACUC-approved protocol at the University of Michigan.

Author contributions

DAG, PCD, and BMS contributed to study concept, design, and data interpretation. DAG, PCD, NMW, and JMWS contributed to data acquisition and analysis. DAG, PCD, and BMS contributed to drafting of the manuscript and figures.

Acknowledgments

This work was supported by National Institute of Neurological Disorders and Stroke grants R01-NS105385 and R21-NS103215 (to BMS) and training grants 5T32GM7863-34 (to DAG) and T32AI007413 (to PCD). BMS is an attending neurologist at the VA Ann Arbor Healthcare System and a Scholar of the A. Alfred Taubman Medical Research Institute. Roman Giger (University of Michigan) provided purified myelin for pHrodo phagocytosis experiments.

Address correspondence to: Benjamin M. Segal, 4013 Biomedical Science Research Building, 109 Zina Pitcher Place, Ann Arbor, Michigan 48109, USA. Phone: 734.615.5635; Email: bmsegal@umich.edu.

1. Kawakami N, et al. The activation status of neuroantigen-specific T cells in the target organ determines the clinical outcome of autoimmune encephalomyelitis. *J Exp Med*. 2004;199(2):185–197.
2. Kroenke MA, Segal BM. Th17 and Th1 responses directed against the immunizing epitope, as opposed to secondary epitopes, dominate the autoimmune repertoire during relapses of experimental autoimmune encephalomyelitis. *J Neurosci Res*. 2007;85(8):1685–1693.
3. Gehrmann J, Banati RB, Kreutzberg GW. Microglia in the immune surveillance of the brain: human microglia constitutively express HLA-DR molecules. *J Neuroimmunol*. 1993;48(2):189–198.
4. Giles DA, et al. Myeloid cell plasticity in the evolution of central nervous system autoimmunity. *Ann Neurol*. 2018;83(1):131–141.
5. Ford AL, Goodsall AL, Hickey WF, Sedgwick JD. Normal adult ramified microglia separated from other central nervous system macrophages by flow cytometric sorting. Phenotypic differences defined and direct ex vivo antigen presentation to myelin basic protein-reactive $CD4^+$ T cells compared. *J Immunol*. 1995;154(9):4309–4321.
6. Miller SD, McMahon EJ, Schreiner B, Bailey SL. Antigen presentation in the CNS by myeloid dendritic cells drives progression of relapsing experimental autoimmune encephalomyelitis. *Ann N Y Acad Sci*. 2007;1103:179–191.
7. Wong GH, Bartlett PF, Clark-Lewis I, Battye F, Schrader JW. Inducible expression of H-2 and Ia antigens on brain cells. *Nature*. 1984;310(5979):688–691.
8. McCarron RM, Wang L, Cowan EP, Spatz M. Class II MHC antigen expression by cultured human cerebral vascular endothelial cells. *Brain Res*. 1991;566(1-2):325–328.
9. Greter M, et al. Dendritic cells permit immune invasion of the CNS in an animal model of multiple sclerosis. *Nat Med*. 2005;11(3):328–334.
10. Prinz M, Erny D, Hagemeyer N. Ontogeny and homeostasis of CNS myeloid cells. *Nat Immunol*. 2017;18(4):385–392.
11. McMenamin PG. Distribution and phenotype of dendritic cells and resident tissue macrophages in the dura mater, leptomeninges, and choroid plexus of the rat brain as demonstrated in wholemount preparations. *J Comp Neurol*. 1999;405(4):553–562.
12. Matyszak MK, Perry VH. The potential role of dendritic cells in immune-mediated inflammatory diseases in the central nervous system. *Neuroscience*. 1996;74(2):599–608.
13. Kivisäkk P, et al. Expression of CCR7 in multiple sclerosis: implications for CNS immunity. *Ann Neurol*. 2004;55(5):627–638.
14. Howell OW, et al. Meningeal inflammation is widespread and linked to cortical pathology in multiple sclerosis. *Brain*. 2011;134(pt 9):2755–2771.
15. Serafini B, et al. Dendritic cells in multiple sclerosis lesions: maturation stage, myelin uptake, and interaction with proliferating T cells. *J Neuropathol Exp Neurol*. 2006;65(2):124–141.
16. Quintana E, et al. DNGR-1(+) dendritic cells are located in meningeal membrane and choroid plexus of the noninjured brain. *Glia*. 2015;63(12):2231–2248.
17. Prodinger C, et al. CD11c-expressing cells reside in the juxtavascular parenchyma and extend processes into the glia limitans of the mouse nervous system. *Acta Neuropathol*. 2011;121(4):445–458.
18. Christy AL, Walker ME, Hessner MJ, Brown MA. Mast cell activation and neutrophil recruitment promotes early and robust inflammation in the meninges in EAE. *J Autoimmun*. 2013;42:50–61.
19. Tsuchida M, et al. Identification of CD4- CD8- alpha beta T cells in the subarachnoid space of rats with experimental autoimmune encephalomyelitis. A possible route by which effector cells invade the lesions. *Immunology*. 1994;81(3):420–427.
20. Reboldi A, et al. C-C chemokine receptor 6-regulated entry of TH-17 cells into the CNS through the choroid plexus is required for the initiation of EAE. *Nat Immunol*. 2009;10(5):514–523.
21. Bartholomäus I, et al. Effector T cell interactions with meningeal vascular structures in nascent autoimmune CNS lesions. *Nature*. 2009;462(7269):94–98.
22. Hawiger D, et al. Dendritic cells induce peripheral T cell unresponsiveness under steady state conditions in vivo. *J Exp Med*. 2001;194(6):769–779.
23. Isaksson M, Lundgren BA, Ahlgren KM, Kämpe O, Lobell A. Conditional DC depletion does not affect priming of encephalitogenic Th cells in EAE. *Eur J Immunol*. 2012;42(10):2555–2563.
24. Yogev N, et al. Dendritic cells ameliorate autoimmunity in the CNS by controlling the homeostasis of PD-1 receptor(+) regulatory T cells. *Immunity*. 2012;37(2):264–275.
25. King IL, Dickendesher TL, Segal BM. Circulating Ly-6C+ myeloid precursors migrate to the CNS and play a pathogenic role during autoimmune demyelinating disease. *Blood*. 2009;113(14):3190–3197.
26. Croxford AL, et al. The cytokine GM-CSF drives the inflammatory signature of $CCR2^+$ monocytes and licenses autoimmunity. *Immunity*. 2015;43(3):502–514.
27. Deshpande P, King IL, Segal BM. Cutting edge: CNS $CD11c^+$ cells from mice with encephalomyelitis polarize Th17 cells and support $CD25^+CD4^+$ T cell-mediated immunosuppression, suggesting dual roles in the disease process. *J Immunol*. 2007;178(11):6695–6699.
28. Mildner A, et al. $CCR2^+$Ly-6Chi monocytes are crucial for the effector phase of autoimmunity in the central nervous system. *Brain*. 2009; 132(pt 9):2487–2500.
29. Anandasabapathy N, et al. Flt3L controls the development of radiosensitive dendritic cells in the meninges and choroid plexus of the steady-state mouse brain. *J Exp Med*. 2011;208(8):1695–1705.
30. Whartenby KA, et al. Inhibition of FLT3 signaling targets DCs to ameliorate autoimmune disease. *Proc Natl Acad Sci U S A*. 2005;102(46):16741–16746.
31. Nakano H, Moran TP, Nakano K, Gerrish KE, Bortner CD, Cook DN. Complement receptor C5aR1/CD88 and dipeptidyl peptidase-4/CD26 define distinct hematopoietic lineages of dendritic cells. *J Immunol*. 2015;194(8):3808–3819.
32. Meredith MM, et al. Expression of the zinc finger transcription factor zDC (Zbtb46, Btbd4) defines the classical dendritic cell lineage. *J Exp Med*. 2012;209(6):1153–1165.
33. Satpathy AT, et al. Zbtb46 expression distinguishes classical dendritic cells and their committed progenitors from other immune lineages. *J Exp Med*. 2012;209(6):1135–1152.
34. Miller JC, et al. Deciphering the transcriptional network of the dendritic cell lineage. *Nat Immunol*. 2012;13(9):888–899.
35. Stober CB, Brode S, White JK, Popoff JF, Blackwell JM. Slc11a1, formerly Nramp1, is expressed in dendritic cells and influences major histocompatibility complex class II expression and antigen-presenting cell function. *Infect Immun*. 2007;75(10):5059–5067.
36. Krause SW, Rehli M, Heinz S, Ebner R, Andreesen R. Characterization of MAX.3 antigen, a glycoprotein expressed on mature macrophages, dendritic cells and blood platelets: identity with CD84. *Biochem J*. 2000;346(pt 3):729–736.
37. Hussain AM, Lee HC, Chang CF. Modulation of CD157 expression in multi-lineage myeloid differentiation of promyelocytic cell lines. *Eur J Cell Biol*. 2000;79(10):697–706.
38. Széles L, et al. TLR3-mediated $CD8^+$ dendritic cell activation is coupled with establishment of a cell-intrinsic antiviral state. *J Immunol*. 2015;195(3):1025–1033.
39. Bettelli E, Pagany M, Weiner HL, Linington C, Sobel RA, Kuchroo VK. Myelin oligodendrocyte glycoprotein-specific T cell receptor transgenic mice develop spontaneous autoimmune optic neuritis. *J Exp Med*. 2003;197(9):1073–1081.
40. Barnden MJ, Allison J, Heath WR, Carbone FR. Defective TCR expression in transgenic mice constructed using cDNA-based alpha- and beta-chain genes under the control of heterologous regulatory elements. *Immunol Cell Biol*. 1998;76(1):34–40.
41. Sherman MA, Weber DA, Jensen PE. DM enhances peptide binding to class II MHC by release of invariant chain-derived peptide. *Immunity*. 1995;3(2):197–205.
42. Slavin AJ, et al. Requirement for endocytic antigen processing and influence of invariant chain and H-2M deficiencies in CNS autoimmunity. *J Clin Invest*. 2001;108(8):1133–1139.
43. Oppmann B, et al. Novel p19 protein engages IL-12p40 to form a cytokine, IL-23, with biological activities similar as well as distinct from IL-12. *Immunity*. 2000;13(5):715–725.
44. Langrish CL, et al. IL-23 drives a pathogenic T cell population that induces autoimmune inflammation. *J Exp Med*. 2005;201(2):233–240.
45. Malawista SE, Gee JB, Bensch KG. Cytochalasin B reversibly inhibits phagocytosis: functional, metabolic, and ultrastructural effects in human blood leukocytes and rabbit alveolar macrophages. *Yale J Biol Med*. 1971;44(3):286–300.
46. Immig K, et al. CD11c-positive cells from brain, spleen, lung, and liver exhibit site-specific immune phenotypes and plastically adapt to new environments. *Glia*. 2015;63(4):611–625.
47. Lucchinetti CF, et al. Inflammatory cortical demyelination in early multiple sclerosis. *N Engl J Med*. 2011;365(23):2188–2197.
48. Jung S, et al. In vivo depletion of $CD11c^+$ dendritic cells abrogates priming of $CD8^+$ T cells by exogenous cell-associated antigens. *Immunity*. 2002;17(2):211–220.
49. Pesic M, Bartholomäus I, Kyratsous NI, Heissmeyer V, Wekerle H, Kawakami N. 2-Photon

imaging of phagocyte-mediated T cell activation in the CNS. *J Clin Invest*. 2013;123(3):1192–1201.
50. Saito Y, Boddupalli CS, Borsotti C, Manz MG. Dendritic cell homeostasis is maintained by non-hematopoietic and T-cell-produced Flt3-ligand in steady state and during immune responses. *Eur J Immunol*. 2013;43(6):1651–1658.
51. Miyazaki T, et al. Mice lacking H2-M complexes, enigmatic elements of the MHC class II peptide-loading pathway. *Cell*. 1996;84(4):531–541.
52. Tompkins SM, Padilla J, Dal Canto MC, Ting JP, Van Kaer L, Miller SD. De novo central nervous system processing of myelin antigen is required for the initiation of experimental autoimmune encephalomyelitis. *J Immunol*. 2002;168(8):4173–4183.
53. Martin WD, Hicks GG, Mendiratta SK, Leva HI, Ruley HE, Van Kaer L. H2-M mutant mice are defective in the peptide loading of class II molecules, antigen presentation, and T cell repertoire selection. *Cell*. 1996;84(4):543–550.
54. Braley TJ, Segal BM. B-cell targeting agents in the treatment of multiple sclerosis. *Curr Treat Options Neurol*. 2013;15(3):259–269.
55. Petereit HF, Moeller-Hartmann W, Reske D, Rubbert A. Rituximab in a patient with multiple sclerosis — effect on B cells, plasma cells and intrathecal IgG synthesis. *Acta Neurol Scand*. 2008;117(6):399–403.
56. Serafini B, Rosicarelli B, Magliozzi R, Stigliano E, Aloisi F. Detection of ectopic B-cell follicles with germinal centers in the meninges of patients with secondary progressive multiple sclerosis. *Brain Pathol*. 2004;14(2):164–174.
57. Magliozzi R, et al. Meningeal B-cell follicles in secondary progressive multiple sclerosis associate with early onset of disease and severe cortical pathology. *Brain*. 2007;130(pt 4):1089–1104.
58. Avalos AM, Ploegh HL. Early BCR events and antigen capture, processing, and loading on MHC class II on B cells. *Front Immunol*. 2014;5:92.
59. Lindert RB, Haase CG, Brehm U, Linington C, Wekerle H, Hohlfeld R. Multiple sclerosis: B- and T-cell responses to the extracellular domain of the myelin oligodendrocyte glycoprotein. *Brain*. 1999;122 (pt 11):2089–2100.
60. Parker Harp CR, et al. B cell antigen presentation is sufficient to drive neuroinflammation in an animal model of multiple sclerosis. *J Immunol*. 2015;194(11):5077–5084.
61. Carbajal KS, et al. Th cell diversity in experimental autoimmune encephalomyelitis and multiple sclerosis. *J Immunol*. 2015;195(6):2552–2559.
62. Huber AK, et al. Dysregulation of the IL-23/IL-17 axis and myeloid factors in secondary progressive MS. *Neurology*. 2014;83(17):1500–1507.
63. Berger T, et al. Antimyelin antibodies as a predictor of clinically definite multiple sclerosis after a first demyelinating event. *N Engl J Med*. 2003;349(2):139–145.
64. Norton WT, Poduslo SE. Myelination in rat brain: method of myelin isolation. *J Neurochem*. 1973;21(4):749–757.